Enhanced Electro-Optic Phase Modulation in InGaAs Quantum Posts at 1500 nm

JaeHyuk Shin, Hyochul Kim, Pierre M. Petroff, and Nadir Dagli, *Fellow, IEEE*

***Abstract*—Electro-optic properties of self assembled InGaAs quantum posts have been studied experimentally. For TE polarization phase modulation enhancement up to 27% over devices containing InGaAs quantum well of the same average composition and thickness was observed indicating significant electro-optic coefficient increase in quantum posts. The measured linear and quadratic electro-optic coefficients of the quantum posts were as high as 17.8×10^{-12} m/V and 49.4×10^{-21} m^2/V^2 at 1500 nm which are more than an order of magnitude larger than those of GaAs.**

***Index Terms*—Optical waveguide components, phase modulation, quantum dots, semiconductor waveguides.**

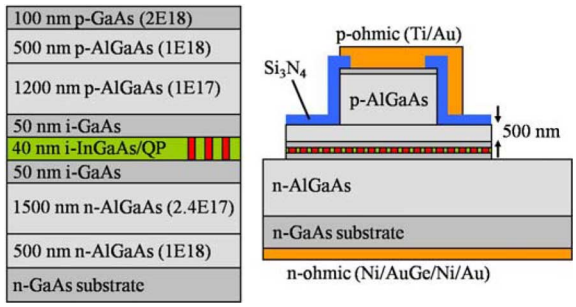

Fig. 1. Details of the epilayer and the cross-sectional profile of the phase modulator. The QPs are schematically shown. Al content is 0.7 for AlGaAs layers.

I. Introduction

NONLINEAR optical and electro-optic materials used in switching and modulation are crucial for realizing photonic integrated circuits. Bulk III–V semiconductors such as GaAs and InP have linear electro-optic (LEO) coefficients much smaller than that of lithium niobate. Advances in crystal growth led to the realization of quantum wells which have enhanced electro-optic effects properties due to quantum confined Stark effect (QCSE) near the excitonic absorption edge [1]. However this improvement typically comes with a bias dependent loss increase. Recently, there has been growing interest in utilizing nanostructures such as self-assembled quantum dots to enhance electro-optic efficiency of semiconductors [2]–[4]. Quantum dots are expected to exhibit enhanced optical nonlinearities and electro-optic effects due to modification in the density of states [5]. Enhancement of phase shift efficiency of multiple layer InGaAs quantum dot (QD) layers over bulk GaAs of about 20%–35% near 1500 nm have been observed [2]–[4]. The extracted linear electro-optic coefficient of the QDs is estimated to be as much as 20 times higher than that of bulk GaAs [3]. This is a significant enhancement making compound semiconductor electro-optic coefficients comparable to that of lithium niobate. Furthermore this improvement comes with little bias dependent loss increase. It is also possible to prepare different types of novel quantum confined structures using self assembly techniques. Quantum posts (QPs) which are stacked QDs connected by short quantum wires are an example of such novel nanostructures [6]–[8]. Currently, there is strong research effort to characterize various physical parameters of quantum posts and to adapt them to various devices such as modulators and memory cells [9]. In this paper, we report on the phase shift enhancement in phase modulators with a single layer of quantum posts (QPs) embedded in the core of the waveguide.

While typical stacked QDs are separated by 35–40 nm thick GaAs spacer layers [3], [4], QPs form a cylinder with composition similar to QDs at the top and bottom. As a result, we expect QPs to have better overlap with the optical mode compared to two stacked QD layers with a GaAs spacer in-between and could lead to higher effective index changes.

II. Material and Device Description

Fig. 1 shows the epilayer detail along with the phase modulator cross-sectional profile. The epilayer was grown on an n-GaAs substrate with MBE. 0.5 μm $Al_{0.7}Ga_{0.3}As(N_D = 1\times10^{18}$ $cm^{-3})$ and 1.5 μm $Al_{0.7}Ga_{0.3}As(N_D = 2.4\times10^{17}$ $cm^{-3})$ layers are grown as the bottom cladding. The 140 nm core layer consists of a 40 nm QP layer imbedded between two 50 nm GaAs spacers. The QPs consists of two self assembled InGaAs QDs connected together by a short InGaAs QW [6]–[8]. The QPs are 40 nm wide and 40 nm high and their areal density is estimated to be $\sim 100/\mu m^2$. 1.2 μm $Al_{0.7}Ga_{0.3}As(N_A = 1\times10^{17}$ $cm^{-3})$ and 0.5 μm $Al_{0.7}Ga_{0.3}As(N_A = 1\times10^{18}$ $cm^{-3})$ layers are grown to form the top cladding. Finally, the structure is capped with a 0.1 μm $GaAs(N_A = 2\times10^{18}$ $cm^{-3})$ layer.

Fabrication starts with RIE etching 2 μm waveguides 1.3 μm deep into the top cladding. 0.3 μm thick Si_3N_4 is evaporated for surface passivation. Slots are opened on top of the waveguide and Ti–Au is evaporated and lifted off to form top

Manuscript received November 05, 2009; revised February 10, 2010. Current version published April 07, 2010. This work was supported in part by the National Science Foundation under Grant ECCS-0702087 and a Defense Advanced Research Projects Agency under STTR grant.

J. Shin and N. Dagli are with the Department of Electrical and Computer Engineering, University of California, Santa Barbara, CA 93106 USA (e-mail: jhshin@ece.ucsb.edu; dagli@ece.ucsb.edu).

H. Kim is with the Department of Physics, University of California, Santa Barbara, CA 93106 USA (e-mail: hckim@physics.ucsb.edu).

P. M. Petroff is with the Department of Electrical and Computer Engineering and Materials Department, University of California, Santa Barbara, CA 93106 USA (e-mail: petroff@engineering.ucsb.edu).

Color versions of one or more of the figures in this paper are available online at http://ieeexplore.ieee.org.

Digital Object Identifier 10.1109/JQE.2010.2044975

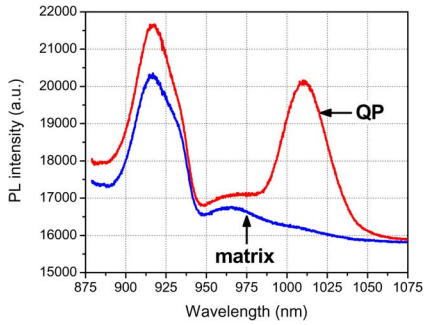

Fig. 2. Photoluminescence spectra of samples with and without QPs at 5 K.

ohmic contacts. 40 μm wide mesas are formed by RIE etching slightly into the bottom cladding to electrically isolate the devices. Ni/AuGe/Ni/Au is blanket evaporated on the bottom of the sample and the contacts are annealed at 430°C for 30 seconds.

The core of the optical waveguide contains QPs which are prepared using controlled deposition of monolayers of GaAs and InAs along with appropriate growth interruptions [6]–[8]. QPs contain higher indium content ($\sim$45%) compared to the InGaAs quantum well ($\sim$12.5%) they are formed in. The top and bottom of the QPs have slightly higher indium content ($\sim$50%). Therefore, the QPs can be thought as two QDs connected by a region of slightly lower indium composition embedded in an InGaAs QW region of even lower indium composition. As a result, their shape and quantum confinement are different from QDs prepared in the same material system. In this work QPs were 40 nm high and 40 nm wide with an areal density about $100/\mu\text{m}^2$. We call the epilayer with the same average InGaAs composition and thickness but without the QPs or QDs the matrix. It is actually possible to obtain both epilayers, i.e., epilayers with QPs and matrix, during the same growth, hence on the same wafer. This is achieved by stopping the rotation of the sample when seed QDs are deposited to form QPs [8]. This approach makes the lower half of the wafer closer to the indium source have a high density of QDs while the upper half has very few QDs. Using this method, samples with high density QPs and no QPs can be obtained at the same time. This approach reduces the possibility of variation in doping level, thickness and composition if the two samples had been grown separately. To verify the variation in QP density, photoluminescence measurements were made on the samples and the results are shown in Fig. 2. The peak near 916 nm corresponds to that of the $In_{0.125}Ga_{0.875}As$ quantum well matrix while that at 1010 nm corresponds to the QPs. The measurement clearly shows that there is very little, if any QDs or QPs in the matrix region. The PL spectra at room temperature do not show the peak due to QPs. However the structure is still identical and indium variation due to presence of QPs exist. For both the QP and matrix layers average indium composition is 12.5%.

III. Experimental Results and Discussion

After the growth and fabrication, the devices were cleaved to 4.5 mm length to form Fabry–Perot phase modulators. Transmission through the Fabry–Perot phase modulators was measured as a function of wavelength at different bias voltages. From the data, index change as a function of bias voltage can be extracted.

In a compound semiconductor contribution of various effects to effective index can be written as

$$\begin{aligned}\Delta n_{\text{TE}} &= \Delta n_{\text{QEO}} + \Delta n_{\text{FC}} \pm \Delta n_{\text{LEO}} \\ \Delta n_{\text{TM}} &= \Delta n_{\text{QEO}} + \Delta n_{\text{FC}}\end{aligned} \tag{1}$$

where Δn_{LEO}, Δn_{QEO}, and Δn_{FC} are the effective index change due to linear electro-optic (LEO), quadratic electro-optic (QEO), and free carrier (FC) related effects. We do not consider the thermo-optic (TO) effect since the *pin* junction is reverse biased and temperature increase due to power dissipation is negligible. Each one of the contributing effects can be calculated using the formulas below:

$$\Delta n_{\text{LEO}}(V) = \frac{1}{2n_{\text{eff}}} \sum_i n_i^4 r_i \int |U|^2 \cdot E(V) dxdy \tag{2}$$

$$\Delta n_{\text{QEO}}(V) = \frac{1}{2n_{\text{eff}}} \sum_i n_i^4 R_i \int |U|^2 \cdot E(V)^2 dxdy \tag{3}$$

$$\begin{aligned}\Delta n_{\text{FC}}(V) = \frac{1}{n_{\text{eff}}} \Bigg(&\sum_i n_i C_{n,i} \int |U|^2 \cdot N(V) dxdy \\ &+ \sum_i n_i C_{p,i} \int |U|^2 \cdot P(V) dxdy \Bigg).\end{aligned} \tag{4}$$

Here, n_{eff} is the effective mode index, n_i is the refractive index, r_i is the linear electro-optic coefficient, R_i is the quadratic electro-optic coefficient, $C_{n,i}$ and $C_{p,i}$ are the electron and hole free carrier coefficients. The subscript i labels regions with different material. U is the normalized optical mode field profile and E is the modulating electrical field. N and P are electron and hole concentrations. LEO effect can either add to or subtract from the other effects depending on the direction of the waveguides with respect to crystal orientation. In our case, waveguides are oriented such that LEO adds to the other effects.

In order to calculate the overall index change given in (1), the optical mode shape, electric field profile, carrier concentration profiles and material coefficients in (2)–(4) must be known accurately. The doping profile must be known to calculate the electrical field profile. The doping profile of the epilayer is found using SIMS analysis. The measured doping level for n and p AlGaAs adjacent to the core was 2.4×10^{17} cm^{-3} and 1×10^{17} cm^{-3} respectively. Accuracy of the doping levels and layer thicknesses can be verified by comparing the measured and calculated CV profiles. Calculation is done with a commercially available software package. These profiles are shown in Fig. 3 and are in very good agreement. The CV profile of devices with and without QPs was virtually identical so only data for devices with QPs is shown.

Once we have confidence in the doping profile we can also calculate the carrier concentrations as a function of bias. The next step is to calculate the optical mode profile. For this calculation all the indexes and thicknesses are known except for

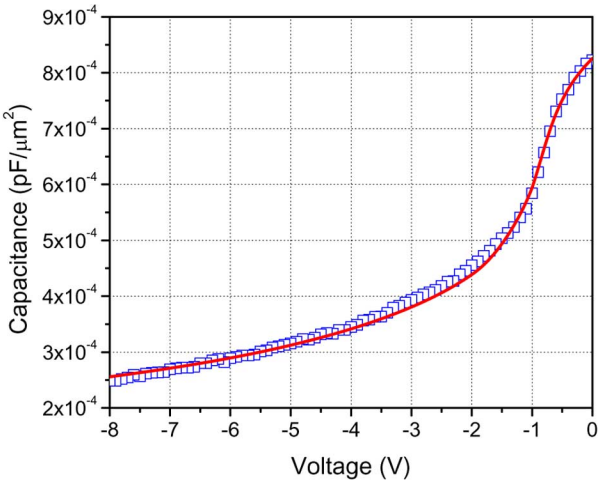

Fig. 3. Measured and calculated capacitance as a function of reverse bias voltage. Open squares and solid line shows measurement data and calculation based on the cross-sectional profile shown in Fig. 1 respectively.

the index of the QP or the matrix layer. For this layer we used the index of GaAs since this layer contains only 12.5% indium and is mostly GaAs. Once the optical mode shape is known it is possible to calculate the overlap integrals in (2)–(4) using the calculated electric field and carrier concentration. The rest of the calculation requires material parameters. While material parameters of GaAs are well known [10]–[14], there is little reliable data for $Al_{0.7}Ga_{0.3}As$ and $In_{0.125}Ga_{0.875}As$. In principle these can be obtained by fitting experimental data to (1). But there are too many unknown coefficients which makes such a fit very difficult. Instead, we perform a comparative analysis by comparing the index change in devices with QPs, Δn_s, to that without QPs, Δn_m. First, we assume that the refractive index of the QP layer is very similar to that of the matrix. Then, we can assume that the optical mode profile is the same with and without QPs. Further, we can assume that the electrical field and doping profiles are the same for both cases since CV measurements are virtually identical for both cases. We do not expect LEO contribution for TM polarization. Then, the difference in index change between devices with and without QPs can be written as

$$\Delta n_s - \Delta n_m\,|_{\mathrm{TM}} = \frac{1}{2n_{\mathrm{eff}}}\left(n_s^4 R_s - n_m^4 R_m\right) \times \int |U_{\mathrm{TM}}|^2 \cdot E^2 dxdy \tag{5}$$

$$\Delta n_s - \Delta n_m\,|_{\mathrm{TE}} = \frac{1}{2n_{\mathrm{eff}}}\left(n_s^4 r_s - n_m^4 r_m\right) \times \int |U_{\mathrm{TE}}|^2 \cdot E dxdy + \frac{1}{2n_{\mathrm{eff}}}\left(n_s^4 R_s - n_m^4 R_m\right) \times \int |U_{\mathrm{TE}}|^2 \cdot E^2 dxdy. \tag{6}$$

Experimentally obtained $\Delta n_s - \Delta n_m|_{\mathrm{TM}}$ and $\Delta n_s - \Delta n_m|_{\mathrm{TE}}$ values are shown in Fig. 4 as a function of bias voltage for phase modulators with and without QPs for both polarizations. We observe that there is an improvement in

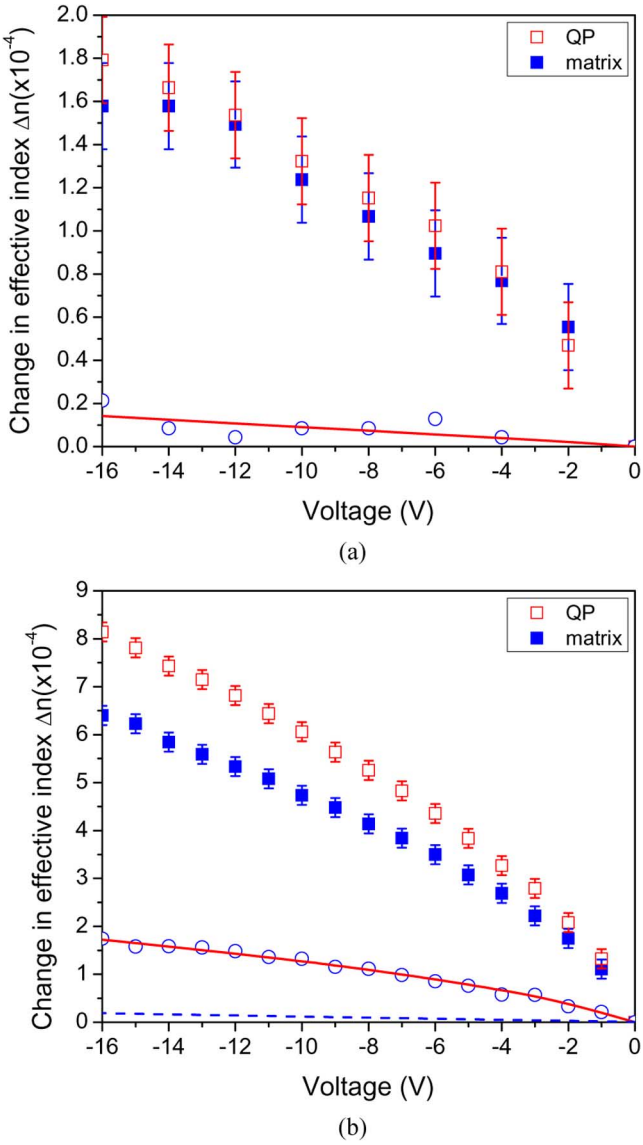

Fig. 4. Index change of modulators with and without QPs as a function of reverse voltage for (a) TM and (b) TE polarization at 1500 nm. Waveguide width is 2 μm. Open circles represents the difference between modulators with and without QPs and the solid lines are fits to data. Dashed line in (b) is the enhancement due to QEO shown in (a).

the index change for both polarizations. For each polarization the open circles are the difference due to the presence of QPs and the solid line is the fit to this data. The improvement is far more significant for TE polarization and is as much as 27%. Based on TM polarization measurements we see the enhancement in the QEO is not significant. This is expected since we are operating at a wavelength far away from the absorption edge of both the QP and matrix layers. Due to significant wavelength dependence of QEO coefficients we expect very little index change contribution due to QEO effect. However the significant enhancement in the index change for the TE polarization leads us to believe that there is significant enhancement in LEO contribution. We can obtain the enhancement in LEO contribution in the following way. For TM polarization $n_s^4 R_s - n_m^4 R_m$ can be obtained by fitting the measurements shown in Fig. 4(a) to (5). As mentioned earlier

this is a very small amount. Assuming the QEO contribution far away from the absorption edge is almost the same for both polarizations, $n_s^4 r_s - n_m^4 r_m$ can be obtained by subtracting the QEO contribution from $\Delta n_s - \Delta n_m|_{\mathrm{TE}}$.

This allows us to quantify the LEO improvement. We observe that index change due to $n_s^4 r_s - n_m^4 r_m$ is an order of magnitude larger than that from $n_s^4 R_s - n_m^4 R_m$ indicating that most of the index change enhancement for TE polarization is from LEO effect. Hence, contribution of QEO to index change is about 10% and error in estimating enhancement due to LEO if QEO is neglected is about 10%.

The relative enhancement of the LEO effect in QPs can be calculated using a fill factor argument as

$$\begin{aligned} n_s^4 r_s - n_m^4 r_m &= F \cdot n_{QP}^4 r_{QP} + (1-F)\, n_m^4 r_m - n_m^4 r_m \\ &= F\left(n_{QP}^4 r_{QP} - n_m^4 r_m\right) \end{aligned} \tag{7}$$

F is the fill factor of the self assembled QPs ($\sim$0.127). Rearranging (7), we obtain

$$\frac{n_{QP}^4 r_{QP}}{n_m^4 r_m} = \frac{\left(n_s^4 r_s - n_m^4 r_m\right)}{F \cdot n_m^4 r_m} + 1. \tag{8}$$

The relative enhancement due to QEO effect can be also calculated in an identical way. Since there is little material information for $In_{0.125}Ga_{0.875}As$ matrix layer, we will use those of GaAs to estimate the relative enhancement of QPs in (8). These values are $n = 3.37$, $r = 1.5 \times 10^{-12}$ m/V, and $R = 4.2 \times 10^{-21}$ m^2/V^2 [14]. Using this approach we obtain $n_{QP}^4 r_{QP}/n_m^4 r_m = 11.85 \pm 1.52$ and $n_{QP}^4 R_{QP}/n_m^4 R_m = 6.4 \pm 4.4$

These numbers are important because they allow us to quantify the improvement independent of the fill factor. There is about an order of magnitude increase in phase shift efficiency for the LEO effect. Since this improvement involves the index of the material one may wonder if there is also a significant improvement in the index. For the enhancement to be due to index alone $n_{QP} \sim 1.78 n_m \sim 6$. Although the index of $In_{0.125}Ga_{0.875}As$ is not known such a high value is unrealistic. Optical propagation loss with and without QPs were identical indicating the band edge is far removed from the measurement wavelength of 1500 nm. From these observations, we can argue that most of the enhancement is due to increase in electro-optic coefficients r and R along with some modest index increase. Further work on measuring the refractive index of $In_{0.125}Ga_{0.875}As$ and QP material is needed to exactly determine the electro-optic coefficients. For comparison, if we use the material parameters of GaAs for the InGaAs matrix, we obtain $r_{QP} = 17.8 \times 10^{-12}$ m/V and $R_{QP} = 49.4 \times 10^{-21}$ m^2/V^2. The enhancement found in QPs is comparable with the improved results on QDs of $n_{QD}^4 r_{QD}/n_m^4 r_m$ of 7–10 [4] and r_{QD} of 34×10^{-12} m/V [3] reported earlier, although in [3] and [4] the possible enhancement in QEO effect is not taken into account.

IV. Conclusions

By imbedding a single quantum post layer in the core of a waveguide, we were able to enhance the TE phase shift efficiency by up to 27% compared to cores with the same average composition and thickness without the QPs. Estimation of the relative enhancement of the LEO and QEO effects in the QPs indicate an order of magnitude improvement for LEO. The extracted LEO and QEO coefficients for the QPs were 17.8×10^{-12} m/V and 49.4×10^{-21} m^2/V^2 respectively. This result is comparable with those obtained from phase modulators with 3–5 layers of QDs imbedded in the core region with respect to bulk GaAs. Phase shift efficiency could be enhanced further by using multiple layers of QPs within the core of the waveguide.

References

[1] D. A. B. Miller, D. S. Chemla, T. C. Damen, A. C. Gossard, W. Wiegmann, T. H. Wood, and C. A. Burrus, "Band-edge electroabsorption in quantum well structures—The quantum-confined stark-effect," *Phys. Rev. Lett.*, vol. 53, pp. 2173–2176, 1984.

[2] S. Ghosh, A. S. Lenihan, M. V. G. Dutt, Q. Qasaimeh, D. G. Steel, and P. Bhattacharya, "Nonlinear optical and electro-optic properties of InAs/GaAs self-organized quantum dots," *J. Vac. Sci. Technol., B*, vol. 19, pp. 1455–1458, Jul.–Aug. 2001.

[3] G. Moreau, A. Martinez, D. Y. Cong, K. Merghem, A. Miard, A. Lemitre, P. Voisin, and A. Ramdane, "Enhanced In(Ga)As/GaAs quantum dot based electro-optic modulation at 1.55 μm," *Appl. Phys. Lett.*, vol. 91, pp. 091118–091118, Aug. 2007.

[4] I. B. Akca, A. Dana, A. Aydinli, M. Rossetti, L. H. Li, A. Fiore, and N. Dagli, "Electro-optic and electro-absorption characterization of InAs quantum dot waveguides," *Opt. Express*, vol. 16, pp. 3439–3444, Mar. 2008.

[5] S. Schmittrink, D. A. B. Miller, and D. S. Chemla, "Theory of the linear and nonlinear optical-properties of semiconductor microcrystallites," *Phys. Rev. B*, vol. 35, pp. 8113–8125, May 1987.

[6] J. He, R. Nötzel, P. Offermans, P. M. Koenraad, Q. Gong, G. J. Hamhuis, T. J. Eijkemans, and J. H. Wolter, "Formation of columnar (In,Ga)As quantum dots on GaAs(100)," *Appl. Phys. Lett.*, vol. 85, pp. 2771–2773, Oct. 2004.

[7] J. He, H. J. Krenner, C. Pryor, J. P. Zhang, Y. Wu, D. G. Allen, C. M. Morris, M. S. Sherwin, and P. M. Petroff, "Growth, structural, and optical properties of self-assembled (In,Ga)As quantum posts on GaAs," *Nano Lett.*, vol. 7, pp. 802–806, Mar. 2007.

[8] H. J. Krenner, C. Pryor, J. He, J. P. Zhang, Y. Wu, C. M. Morris, M. S. Sherwin, and P. M. Petroff, "Growth and optical properties of self-assembled InGaAs quantum posts," *Physica E*, vol. 40, pp. 1785–1789, Apr. 2008.

[9] H. J. Krenner, C. E. Pryor, J. He, and P. M. Petroff, "A semiconductor exciton memory cell based on a single quantum nanostructure," *Nano Lett.*, vol. 8, pp. 1750–1755, Jun. 2008.

[10] J. G. Mendozaalvarez, L. A. Coldren, A. Alping, R. H. Yan, T. Hausken, K. Lee, and K. Pedrotti, "Analysis of depletion edge translation lightwave modulators," *J. Lightwave Technol.*, vol. 6, pp. 793–808, Jun. 1988.

[11] J. Faist and F. K. Reinhart, "Phase modulation in GaAs AlGaAs double heterostructures.1. Theory," *J. Appl. Phys.*, vol. 67, pp. 6998–7005, Jun. 1990.

[12] J. Faist and F. K. Reinhart, "Phase modulation in GaAs AlGaAs double heterostructures. 2. Experiment," *J. Appl. Phys.*, vol. 67, pp. 7006–7012, Jun. 1990.

[13] S. S. Lee, R. V. Ramaswamy, and V. S. Sundaram, "Analysis and design of high-speed high-efficiency GaAs-AlGaAs double-heterostructure wave-guide phase modulator," *IEEE J. Quantum Electron*, vol. 27, pp. 726–736, Mar. 1991.

[14] C. A. Berseth, C. Wuethrich, and F. K. Reinhart, "The electrooptic coefficients of GaAs—Measurements at 1.32 μm and 1.52 μm and study of their dispersion between 0.9 μm and 10 μm," *J. Appl. Phys.*, vol. 71, pp. 2821–2825, Mar. 1992.

JaeHyuk Shin received the B.S. degree in inorganic materials engineering from Seoul National University, Seoul, Korea, in 1999, and the Ph.D. degree in materials from the University of California at Santa Barbara, Santa Barbara, CA, in 2007.

He is currently working as a Postdoctoral Researcher in the Electrical and Computer Engineering Department, University of California at Santa Barbara. His current interests are the design, simulation, fabrication and analysis of high-bandwidth low-drive voltage modulators for fiber-optic communications.

Hyochul Kim received the B.S. degree in physics from Korea Advanced Institute of Science and Technology, Daejeon, Korea in 2001, and the Ph.D. degree in physics from the University of California at Santa Barbara in 2009.

He is currently working as a Postdoctoral Researcher in the Physics Department at the University of California at Santa Barbara. His current interests are design, growth, fabrication and optical analysis of semiconductor quantum dot–microcavity systems.

Pierre M. Petroff graduated from the University of California at Berkeley in 1967.

He joined ATT Bell Laboratories in 1971 after a Postdoc at Cornell University, Ithaca, NY. He has been a faculty member at the University of California at Santa Barbara in the Materials Department and Electrical and Computer Engineering Department since 1986. His group has been focused on the growth, device applications and spectroscopy of quantum wires and quantum dots in compounds semiconductors. He holds more than 15 patents and has authored or coauthored over 500 publications.

Dr. Petroff was the recipient of a Fulbright Fellowship and a Humboldt Senior Research Award. He is a Fellow of the APS and the AAAS.

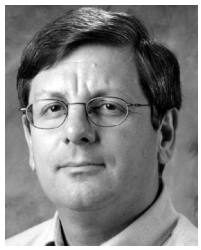

Nadir Dagli (S'77–M'87–SM'04–F'06) received the Ph.D. degree in electrical engineering from the Massachusetts Institute of Technology (MIT), Cambridge, MA, in 1986.

After graduation he joined the electrical and computer engineering department at University of California at Santa Barbara, where he is currently a Professor. His current interests are design, fabrication and modeling of guided-wave components for optical integrated circuits, ultrafast electro-optic modulators, WDM components and photonic nanostructures. He has served on and chaired many technical program and other professional committees. He was the Editor-in-Chief of IEEE PHOTONICS TECHNOLOGY LETTERS during 2000–2005 and an elected member of the IEEE LEOS Board of Governors during 2003–2005.